JOURNAL OF MATERIALS SCIENCE 33 (1998) 2079–2085

Study by a modified scanning electron microscope fractography of hydrogenation process in vapour grown carbon fibres

A. MADROÑERO
CENIM, Avda Gregorio del Amo 8, 28040 Madrid, Spain

M. VERDÚ
CIDA, C/Arturo Soria 289, 28033 Madrid, Spain

J. P. ISSI,
Unité de Physico-Chimie et de Physique des Materiaux, Université de Louvain la Neuve, B-1348 Belgium

J. MARTIN-BENITO ROMERO, C. BARBA
Centro de Microscopia Electrónica de la Universidad Complutense, Ciudad Universitaria, 28040 Madrid, Spain

The present paper intends to study the microstructure of vapour grown carbon fibres (VGCF), whose fracture depends on the breaking mode, as it was stated. Before being examined, transversal sections of fibres were etched, using an argon ion beam, aiming to remove a thin surfacial layer, then seriously altered by the failure process. After that, based upon the results of the scanning electron microscopy (SEM) examination, it can be established that the inner core of as-grown VGCF is constituted by a Rowland's structure. Although differentiated crystals do not exist in the cortical phase, the boundary between the core and the latter phase is clearly observable. After that, an overhydrogenation process took place as a result of an annealing of the fibres in a hydrogen atmosphere.

The microstructure had been, by then, slightly modified. In the inner core, not only the gap width between crystals had been modified but the boundary between catalytical and pyrolytical phases had vanished as well. As a consequence of such modifications, the fibres Young's modulus increases and their failure strain diminishes, in a similar manner as the mechanical properties of current ex-polyacrylonitrile (PAN) carbon fibres are altered by graphitization, during a graphitizing process.

1. Introduction

Vapour grown carbon fibres (VGCF) are a non-continuous fibre having very attractive mechanical properties, tensile strength about 2.9 GPa and a Young's modulus as 240 GPa [1], and a production cost of about 10$/kg [2].

A hydrocarbon vapour must be combined both with a catalyst source (e.g. iron particles) and hydrogen, if the production of VGCF is aimed. In a proper temperature environment, the hydrocarbon gas decomposes, yielding carbon which dissolves in catalytic particles and initiates the growth of primary fibres, that are thickened to a diameter of several microns by additional carbon depositions. Such fibres can be subsequently heat treated, in order to enhance their crystal structure and properties [3].

VGCF grown by a vapour–liquid–solid mechanism [4] are used in the present work. Because of the growing model, the catalytic inner core of VGCF is made up by coronene $C_{24}H_{12}$, that it is characterized by a 5% hydrogen content. This primary filament is coated with a pyrolytic carbon deposit that stores about 2% hydrogen [5].

Both of these sorts of composition give to VGCF a duplex structure, a core made of a catalytic phase having a strength of 2.9 GPa and a weaker cortical pyrolytic phase, with 940 MPa.

This is not very uncommon; in some ways this two-phase structure is not very different to the duplex structure described by Bennet *et al.* [6] for some ex-polyacrylonitrile (PAN) fibres "a thin outer shell in which there is an increase of the size of the carbon atomic layers L_a, the thickness of the carbon layer stack L_c, and the radius of curvature of the layers r".

But in the case of VGCF, such strength differences must be pondered in terms of their dissimilar hydrogen content, because according to Zou *et al.* [7], it established a relationship between hydrogen content and hardness for αC : H material, with some influence

of the deposition process, that is similar in the cortical phase of VGCF to many αC : H deposits.

The aim of the present work is to explore the possibility of converting the cortical phase of VGCF in a harder material, to improve the strength of the whole fibre. From the point of view of industrial production of VGCF it would be very interesting, because the manufacturer have the possibility to produce very thick VGCF, very easily. As the thickness of the pyrolytical cortical deposit increases in the time with known kinetics [8], using long production process for VGCF manufacturing, we can increase the fibre production in grams of VGCF per batch. So if a further conversion of the cortical phase strength produces the optimal strength of the whole fibre, the overhydrogenation of VGCF appears to be very beneficial, from the point of view of costs.

In the present study, the overhydrogenation consisted of an annealing of the fibres in an hydrogen atmosphere in half an hour. In accordance to Nyaiesh and Nowak [9], our process of overhydrogenation by diffusion was performed at 550 °C, in the temperature range where there is a preferential window in the sorption–desorption process of the hydrogen in the carbon.

2. Experimental procedure

In some technical literature, studies exist of sections of ex-PAN fibres performed by transmission electron microscopy (TEM) observations of transversal thin slides. The preparation technique for TEM samples of carbon ex-PAN fibres is known [10]: "cross and longitudinal sections of fibres embedded in Polarbed epoxy resin were prepared by ultramicrotomy, which allows section thicknesses of 50 to 100 nm to be obtained". In a previous work [11] this preparation technique has been proven for TEM study of VGCF.

Electron diffraction images are referred to in several papers [12] and show cylindrical, not very continuous layers, parallel to the fibre axis in accordance with the ribbon model [13].

Nevertheless, in the common technical literature, the current operation mode that is followed when the observation of the internal grain of these fibres is aimed consists of a scanning electron microscope (SEM) observation of the transversal section of a cut fibre. The appearance of the cleaved catalytic core [1] that was observed was labelled as "trunk tree". However, according to our experience, many of the features of the fracture of VGCF depend on the breaking mode. In Fig. 1a, for instance, the fibre (cut by scissors) shows few, although very thick layers. In Fig. 1b (cut by scissors as well) the cortical layer of the fibre appears to be separated from the core.

By contrast, in Fig. 1c the tensile failure does not produce core-cortical phase debonding. In pyrolytic carbon features like coarse rings are produced. As shown in Fig. 2a, a fibre failed in non-tensile test shows a very occasional adhesion to its surrounding fibres, and that allows us to identify the cortical vitreous appearance, very frequent in pyrolytic carbons,

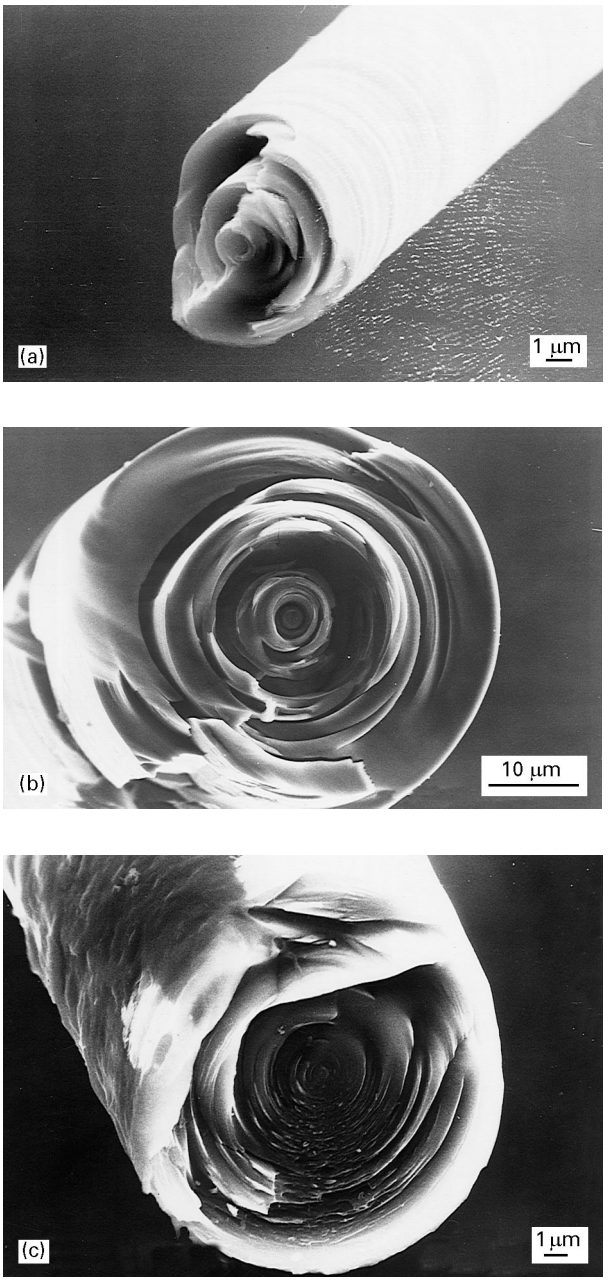

Figure 1 Influence of the breaking mode on fracture of VGCF: (a) cut by scissors; (b) cut by scissors; (c) Tensile failure.

as the fracture appearance of the cortical phase. In Fig. 2b, a highly magnified picture of the same fracture shows small segments of the outermost layers instead of a vitreous fracture, indicating that a laminar microstructure could have been formed during the tensile failure process.

So, if the SEM observation of a fracture depends on the breaking process, it would be necessary to check other ways. The selected procedure in this work is as follows. After being imbibed in bakelite, the samples of our fibre were cut with a diamond wheel, and later polished with alumina and diamond paste (1 μm). In order to avoid the possibility of an anamorfosis perhaps due to the distortions to the microstructure of the fibre during the failure process was followed by the a slight erosion by a mild ion beam etching. The equipment that was used, a Microetch System (model ME-601), had been manufactured by Veeco. The transversal

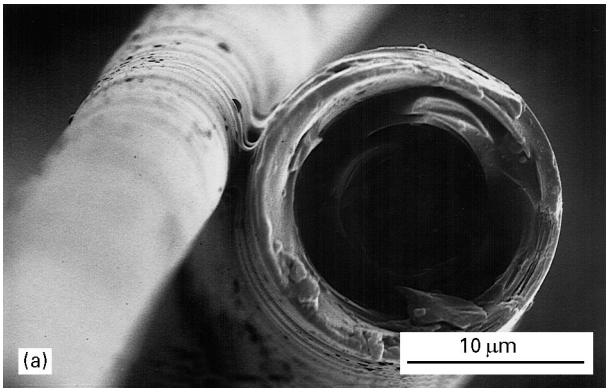

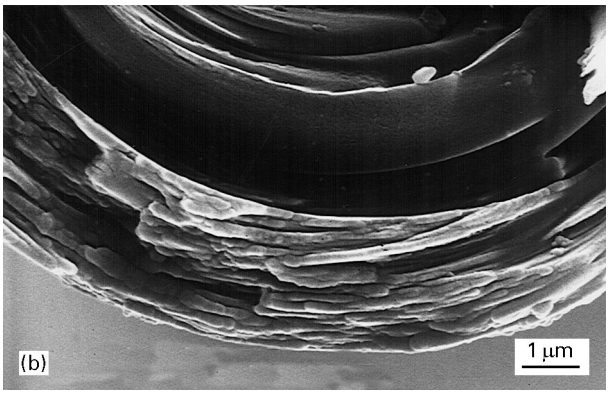

Figure 2 Effect of tensile failure on pyrolytic phase fracture: (a) inner and outer phases; (b) pyrolytic outer layer showing laminar grain.

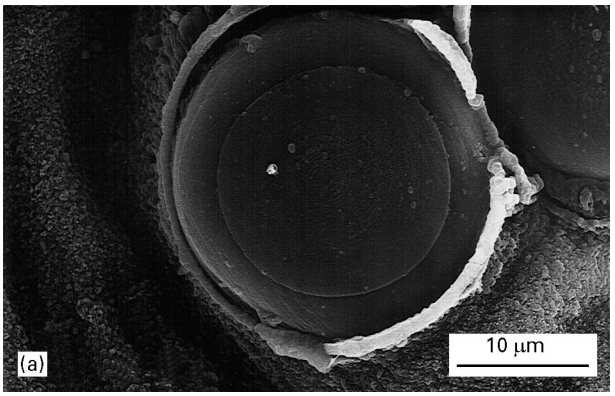

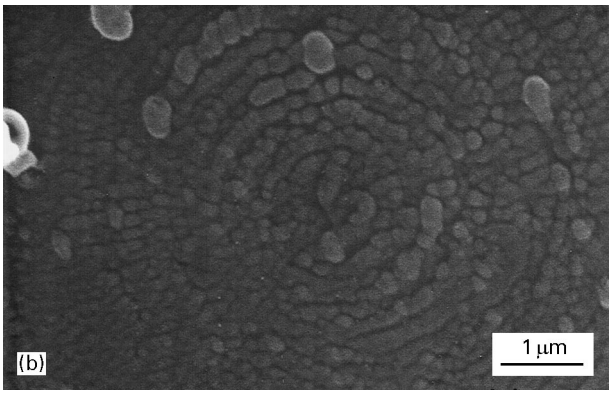

Figure 3 Transversal section of an eroded fibre: (a) complete section; (b) inner core.

section of the fibre withstands a mild erosion by a highly linear argon beam, previously extracted from a plasma source. The intensity of the ion beam was 300 mA, the incident angle 30° and the etching time was 14 min. When such a process of erosion has been performed, this dry etching showed the internal grain of the specimens, being unaltered, without any anamorphosis. Of course, if the iron etching was stronger, the fibre section would show a burred topography.

Two types of VGCF were prepared and labelled as thin and thick aiming to check the influence of over-hydrogenation upon them. Using an atmosphere of 30% CH_4 and 70% H_2, and a working temperature of 1333 K, two batches of VGCF were made. The metallic salt dissolution that was used as a catalyst source for the thick fibres was $(NO_3)_3Fe$, whereas the one used for the thin ones was $(NO_3)_3Fe$ plus $TiO.SO_4$. The enlargening time was 20 min for thin fibres and 45 min for the thick ones. The average thickness of the fibres was 7.5 μm for the former fibres and 8.5 μm for the latter.

3. Results and discussion

3.1. Influence of the hydrogen diffusion on the microstructure of VGCF

At first we made a SEM observation of VGCF microstructure as-grown, previous to annealing in hydrogen atmosphere. In Fig. 3a the core of a complete section of a surfacially eroded VGCF shows a polycrystalline state whereas the cortical phase has a more

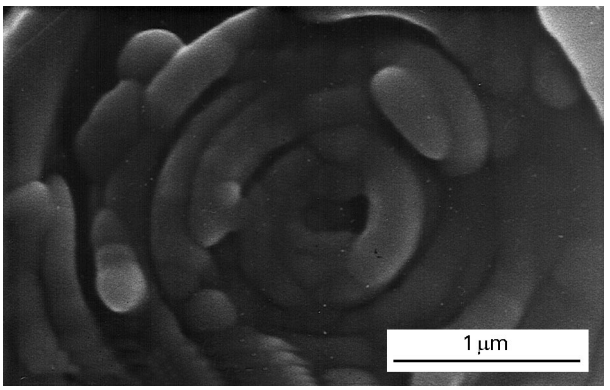

Figure 4 Inner core of a fibre cut by scissors.

isotropic appearance. The more pronounced wear in the cortical phase is clearly influenced by the unequal hardness; that is due to the different degree of preferred orientation in the crystallites of both phases [11]. In Fig. 3b it is possible to see that the tree trunk grain is not constituted by parallel and regular rings. It is formed by a circular, mosaic grain, according to the ribbon structure.

Fig. 4 shows a transversal fibre fracture, in a non-eroded section, having an appearance of short segments of circular furrows. The bean-shaped hollow channel that is placed near the centre of the fibre is not due to the displacement of the fibre seed, as was stated in Tibbets's model for fibre growing [1] following the carbide formation mechanism. This bean-shaped channel is a consequence of the shrinkage caused by the solidification process of the liquid drop of coronene, in accordance with the VLS model

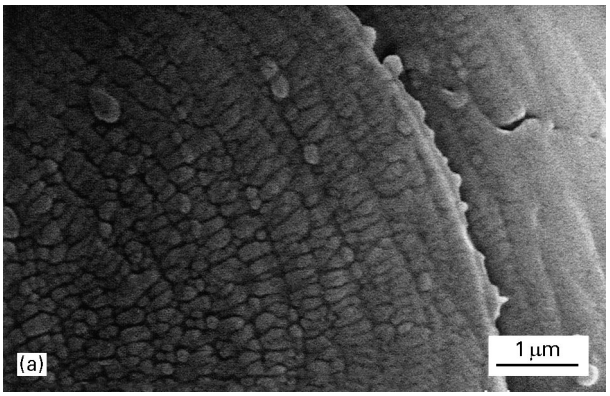

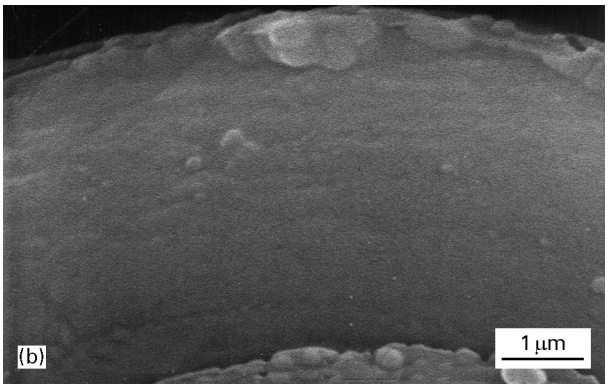

Figure 5 Innner core, interface and cortical phases in an eroded section of an as grown fibre: (a) boundary catalytic–pyrolytic phases; (b) pyrolytic outer phase.

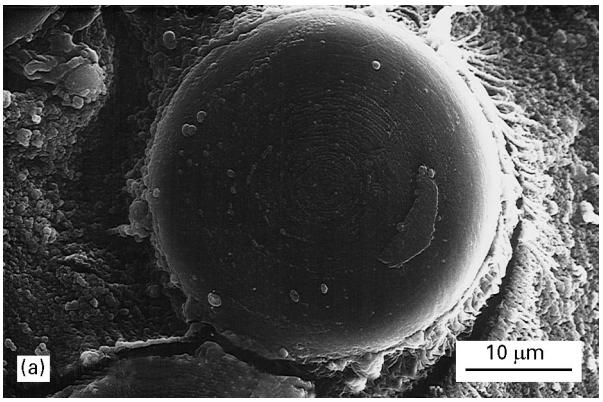

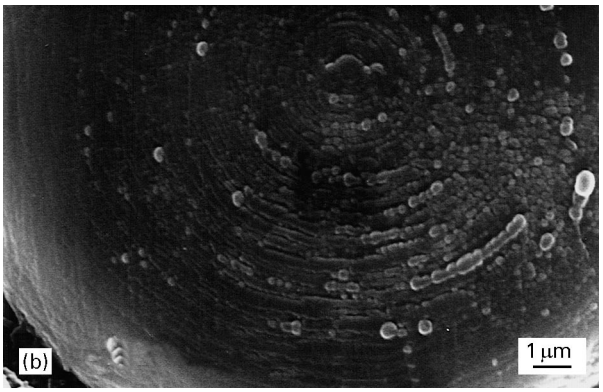

Figure 6 Microstructure of an hydrogenated fibre (non-eroded section): (a) complete transversal section; (b) microstructure gradient in transversal section.

[4]. Nevertheless, these holes that result from the contraction of a melted drop during the solidification process, are hardly ever observed.

However, the most relevant aspect of as-grown fibres is the noticeable boundary between the core and the pyrolytical carbon of the cortical area, as it is shown in Fig. 5a; the bulk cortical phase appears to have a glassy nature, and only the narrow path in contact with the boundary is slightly converted to a core phase appearance. It must be caused by diffusion of hydrogen from the core (5%) toward the outer layer (2%).

The difference between the crystallinity of pyrolytic and catalytic carbons is also remarkable. In Fig. 5b the glassy appearance of the cortical phase is shown, instead of the mosaic structure of the catalytic core.

Lamouroux *et al.* [14] studied the interphase between pyrolytic carbon, deposited from methane, and T300 (an ex-PAN) fibre. The temperature deposition was between 1273 and 1373 K, in a similar mode as was done in the VGCF studied in this work. Then, the interphase thickness is about 0.02 μm. The difference between Lamoroux's results and Fig. 5a can be interpreted in terms of different grain in the surface of T300 fibre and primary catalytic filament of VGCF. The surface of T300 is a porous outer zone. And the surface of the primary catalytic filament is a cylindrical interface caused by a solidification of a mobile molted drop, according to the VLS model [4].

Following the same technique, both for sample mounting and argon ion dry etching, and after enduring an annealing in a hydrogen atmosphere, several samples of VGCF were prepared as it was described above.

In Fig. 6 the cortical area has a smooth aspect, but in Fig. 7 the evolution from glassy to mosaic structure is clearly visible. So, the effect of hydrogenation is to promote the outer layer conversion (compare Figs 7b and 5a) and this feature is displayed by the dry etching (compare Figs 6b and 7b).

The gap between crystals, which is larger in overhydrogenated fibres, being the only difference between Fig. 3b and Fig. 7a, suggests that a local inflation process [15] takes place, as is shown in Fig. 8, i.e. the hydrogen increases the pressure in the accumulation sites (in Condon and Schober's model [15] the pressure may reach 5 GPa).

Consequently, on the one hand hydrogen is introduced in the cortical phase, specially in easily accessible outer places for the external hydrogen via diffusion from the atmosphere, it being the explanation for the bent parallel layers shown in Fig. 2b. On the other hand, the tensile behaviour of overhydrogenated VGCF must be more brittle than the one of as-grown fibres, because the increased hydrogen content enhances the splitting of the cortical phase during the tensile process.

3.2. Influence of overhydrogenation on mechanical properties of VGCF

Although the tensile strength of thin and thick fibres is different, in both cases we can use the same mechanical model.

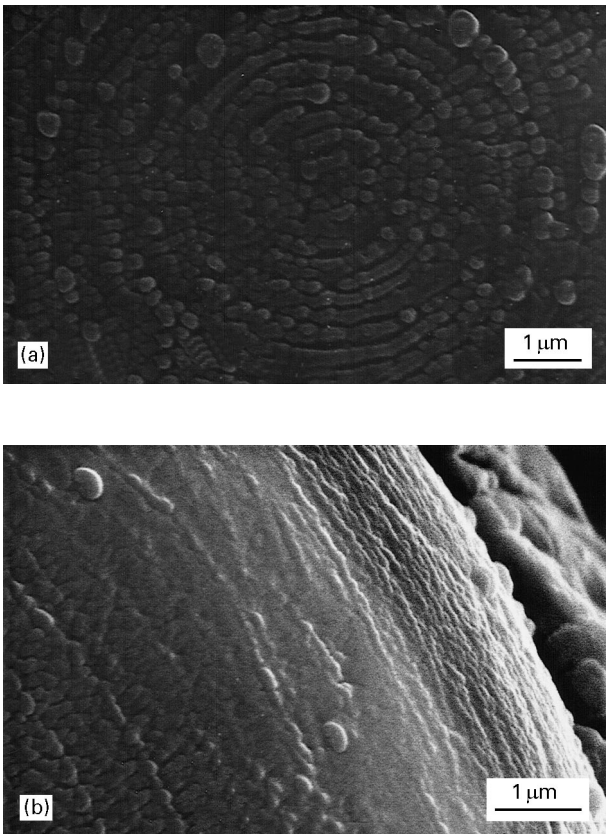

Figure 7 Phases in an eroded section of an hydrogenated fibre: (a) inner core; (b) cortical area.

A stress–strain plot of one sample representative of each two kinds of fibres is represented in Figs 9 and 11. Now we can use Equation 1 taken from [4]:

$$\sigma = \sigma_1 \frac{\pi r^2}{\pi R^2} + \sigma_2 \frac{\pi(R^2 - r^2)}{\pi R^2} = \left(\frac{r}{R}\right)^2 (\sigma_1 - \sigma_2) + \sigma_2 \quad (1)$$

where σ is the fibre tensile strength, $\sigma_1 = 2860$ MPa is the strength of the core phase (radius R) and $\sigma_2 = 940$ MPa is the strength of the cortical area (radius r). If in Equation 1 we put $R = 3.73$ μm according Fig. 9, we obtain $r = 3.51$ μm for thin fibres, but, if as in Fig. 11 we take R as 4.23 μm, we obtain $r = 2.66$ μm.

The purpose of using a simple iron salt to produce small seeds was to procure a very thick pyrolytic coating in fibres, such as the ones shown in Fig. 11, even though it meant having a thin core and implied a long manufacturing time. Similarly, when an Fe–Ti salt and short manufacturing were involved, we were procuring a fibre mainly constituted by core phase.

The comparison between Figs 9 and 11 states that the addition of pyrolytic carbon to the core implies a dismissal both of the tensile strength and the elastic modulus of the fibre. In both cases, however, the failure strain is about 0.8%.

The tensile behaviour of VGCF, once they have been annealed in hydrogen after the manufacturing, is as described in Figs 10 and 12. The failure strength, which corresponds to a brittler core, is now about 0.4%. The similarity between the fibres

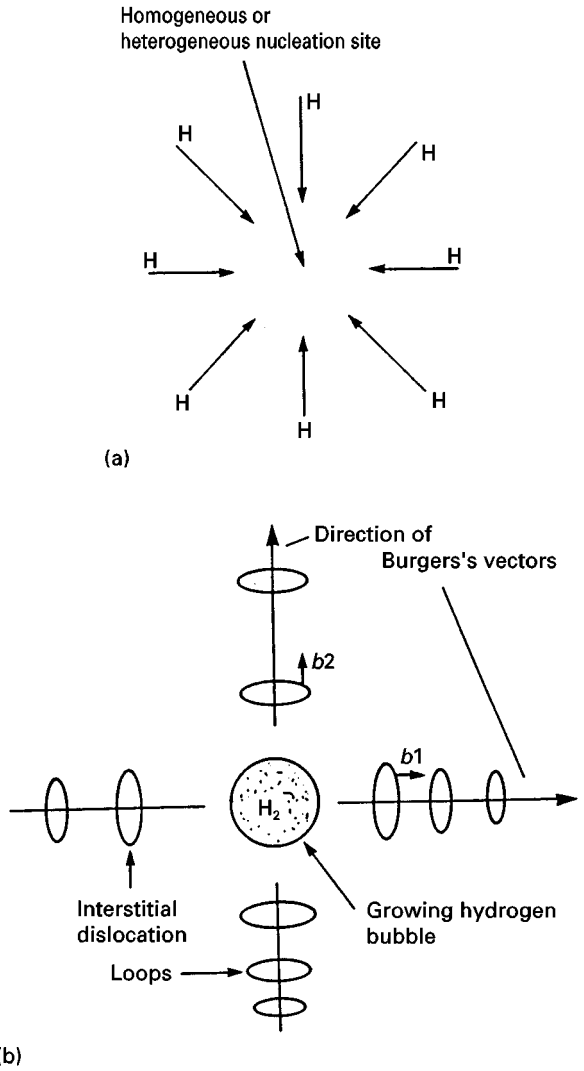

Figure 8 Local punching process due to an excess of hydrostatic pressure. From [15]. (a) Accumulation of hydrogen; (b) growing by hydrogen absorption.

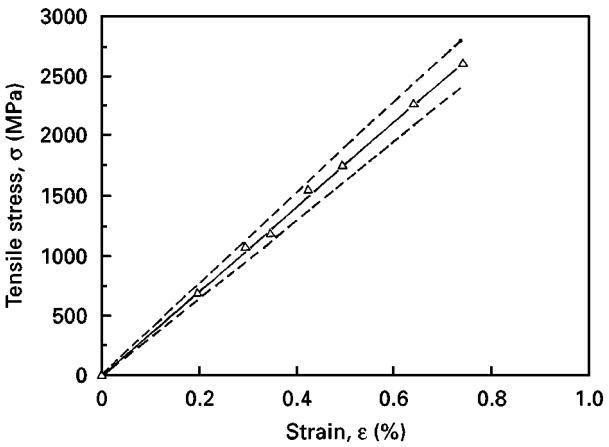

Figure 9 Tensile test of thin fibres as grown. Fibre thickness 7.46 μm, Young's modulus 350 GPa, $\sigma = 3502\varepsilon$.

that correspond to Figs 10 and 12 could be explained in relation to the thickness of fibres. In the case of thick fibres, the overhydrogenation was rather incomplete because of the extreme thickness of the pyrolytic coating.

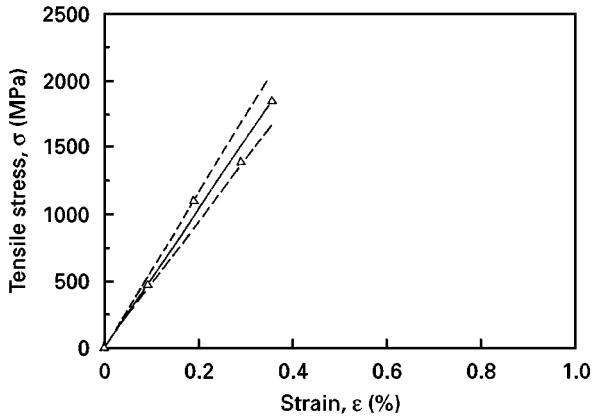

Figure 10 Tensile test of overhydrogenated thin fibres. Fibre thickness 7.50 μm, Young's modulus 35 GPa, $\sigma = 5350\varepsilon$.

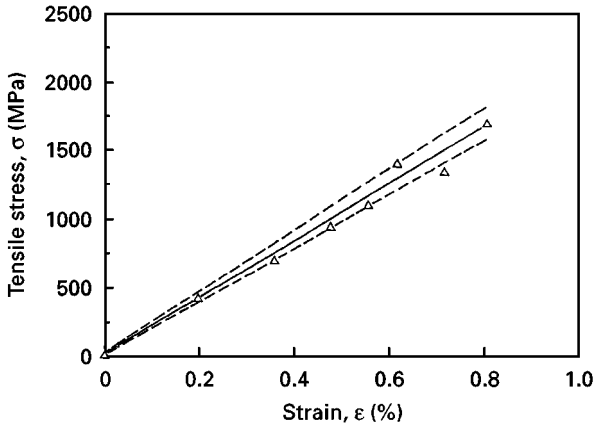

Figure 11 Tensile test of thick fibres as grown. Fibre thickness 8.45 μm, Young's modulus 211 GPa, $\sigma = 2111\varepsilon$.

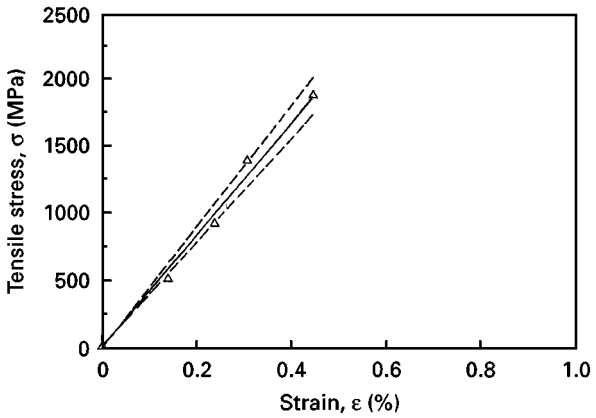

Figure 12 Tensile test of overhydrogenated thick fibres. Fibre thickness 8.38 μm, Young's modulus 421 GPa, $\sigma = 4214\varepsilon$.

In comparison with the graphitization process, an overhydrogenated VGCF is half way between as-grown and graphitized. After a heat treatment at 2373 K [16], VGCF have a tensile strength of $3 \sim 7$ GPa, a Young's modulus of $360 \sim 600$ GPa and a failure strain of about 0.5%. In Fig. 10 we can find a tensile strength about 2 GPa, a Young's modulus of 535 GPa and 0.4% as strain failure.

As a final comment, it is possible to say that overhydrogenation is a good way to achieve reasonably good fibres without following a process that may be as expensive as one of graphitizing at a high temperature. The excessively short failure strain that is produced by the overhydrogenation could perhaps be avoided in the future by means of a steeped hydrogen absorption and/or absorption/desorption cycles. However, much extensive research must still be performed in order to achieve such aims.

4. Conclusions

After the discussion above it would be reasonable to admit that:

1. If a proper observation of the microstructure of VGCF is wanted, it is necessary to avoid the distortion imposed by every failure process. A surfacial erosion, performed for example by argon ion dry etching, after a cut with a diamond wheel, would be an excellent procedure.
2. In as-grown VGCF the core has a circular mosaic structure, according to the ribbon structure.
3. The boundary between the pyrolytic and the catalytic carbon is clearly visible in as-grown fibres.
4. An overhydrogenation means an expansion of the ribbon structure for a conversion of the cortical phase onto lamellar/mosaic structure.
5. From the point of view of the mechanical properties of VGCF, overhydrogenation is a process that may partially compete with graphitizing.

Acknowledgements

The present work was realized as an action of the Human Capital and Mobility Network "Products and Applications of Vapour Grown and other Ceramic Fibres and Filaments" (Contract CHRX-CT-94-0457). We thank the Commission of the European Communities for their financial help in performing this study.

References

1. G. G. TIBBETTS, *Carbon* **27** (1989) 745.
2. S. BECK, in "How to apply advanced composites technology", ASM International Congress, Dearborn, MI, 1988, (American Society for Metals, Metals Park, OH, 1988) p. 467.
3. G. P. DAUMIT, *Carbon* **27** (1989) 759.
4. A. MADROÑERO, *J. Mater. Sci.* **30** (1995) 2061.
5. A. MADROÑERO and M. VERDÚ, *Carbon* **33** (1995) 247.
6. S. C. BENNET and D. J. JOHNSON, *ibid* **17** (1990) 25.
7. J. W. ZOU, K. REICHELT, K. SCHMIDT and B. DISCHLER *J. Appl. Phys.* **65** (1989) 3914.
8. P. GADELLE, in: "Carbon fibres, filaments and composites", edited by J. L. FIGUEIREDO, C. A. BERNARDO, R. T. K. BAKER and K. J. HÜTTINGER, NATO Adv. Stud. Inst. Ser., Series E, 177, (1990) 87.
9. A. R. NYAIESH and W. B. NOWAK, *J. Vac. Sci. Technol.* **A1** (1983) 308.
10. A. DEURBERGUE and A. OBERLIN, *Carbon* **30** (1992) 981.
11. A. MADROÑERO, M. VERDÚ, E. ARIZA, W. BRANDL and C. BARBA, *J. Mater. Sci.* **31** (1996) 6189.
12. G. G. TIBBETTS, M. ENDO and C. P. BEETZ, *SAMPE J.* **22** (1986) 30.

13. A. FOURDEUX, R. PERRET and W. J. RULAND, in "Carbon Fibres, Their Composites and Applications". (The Plastic Institute, London, 1971) p. 57.
14. F. LAMOUROUX, X. BOURRAT, R. NASLAIN and J. SEVELY, *Carbon* **31** (1993) 1273.
15. J. B. CONDON and T. SCHOBER, *J. Nucl. Mater.* **207** (1993) 1.
16. R. L. JACOBSEN, "Control of Physical Properties Variation in Vapour Grown Carbon Fibres", Report SBIR Program, (National Science Foundation, USA, 1994).

Received 2 January
and accepted 17 December 1997